National Institute of Standards & Technology

Report of Investigation

Reference Material® 8013

Gold Nanoparticles, Nominal 60 nm Diameter

This Reference Material (RM) is intended primarily to evaluate and qualify methodology and/or instrument performance related to the physical/dimensional characterization of nanoscale particles used in pre-clinical biomedical research. The RM may also be useful in the development and evaluation of in vitro assays designed to assess the biological response (e.g., cytotoxity, hemolysis) of nanomaterials, and for use in interlaboratory test comparisons. RM 8013 consists of nominally 5 mL of citrate-stabilized Au nanoparticles in an aqueous suspension, supplied in hermetically sealed pre-scored glass ampoules sterilized by gamma irradiation. A unit of RM 8013 consists of two 5 mL ampoules. The suspension contains primary particles (monomers) and a small percentage of clusters of primary particles.

Expiration of Value Assignment: The reference values for **RM 8013** are valid, within the measurement uncertainty specified, until **25 October 2018**, provided the RM is handled and stored in accordance with the instructions given in this report (see "Notice and Warning to Users"). This report is nullified if the RM is damaged, contaminated, or otherwise modified.

Maintenance of RM: NIST will monitor this RM over the period of its validity. If substantive technical changes occur that affect the reference values before the expiration of this report, NIST will notify the purchaser. Registration (see attached sheet or register online) will facilitate notification.

The overall technical coordination for material procurement, processing and measurement activities was conducted by V.A. Hackley and J.F. Kelly of the NIST division formerly known as the Ceramics Division.

Reference and informational value measurements were performed at NIST by the following: T.A. Butler, R. Case, K.W. Pratt, L.C. Sander, and M.R. Winchester of the NIST division formerly known as the Analytical Chemistry Division; A.J. Allen, T.J. Cho, J. Grobelny, V.A. Hackley, D.-I. Kim and P. Namboodiri of the NIST division formerly known as the Ceramics Division; J.E. Bonevich and A.J. Shapiro of the NIST division formerly known as the Metallurgy Division; M.L. Becker, D.L. Ho, A. Karim and B.M. Vogel of the NIST division formerly known as the Polymers Division; B. Ming and A.E. Vladár of the NIST division formerly known as the Precision Engineering Division; L.F. Pease III, M.J. Tarlov, D.H. Tsai, M.R. Zachariah and R.A. Zangmeister of the NIST division formerly known as the Process Measurements Division.

Statistical consultation on measurement design and analysis of the reference value data were performed by A.I. Avilés of the NIST Statistical Engineering Division.

Additional technical and coordination aspects were provided by the following: R.F. Cook, W.K. Haller and D.L. Kaiser of the NIST Materials Measurement Science Division.

Support aspects involved in the issuance of this RM were coordinated through the NIST Office of Reference Materials.

RM 8013 was developed at the request of the National Cancer Institute (NCI). Development and production costs were subsidized by NCI.

John A. Small, Chief
Materials Measurement Science Division

Gaithersburg, MD 20899
Report Issue Date: 24 July 2015
Report Revision History on Last Page

Robert L. Watters, Jr., Director
Office of Reference Materials

Reference Values: Reference values are a best estimate of the true value provided by NIST where all known or suspected sources of bias have not been fully investigated by NIST [1]. Dimensional reference values (mean particle diameter in solution, as an aerosol and deposited on a substrate) are reported and are based on the following measurement techniques: atomic force microscopy (AFM), scanning electron microscopy (SEM), transmission electron microscopy (TEM), electrospray-differential mobility analysis (ES-DMA), dynamic light scattering (DLS) and small-angle x-ray scattering (SAXS). The corresponding reference values and expanded uncertainties are provided in Table 1. A synopsis of the methods used to generate reference values is provided starting on page 7. The measurands are the particle size based on the indicated methods. The reference values are metrologically traceable to the SI unit for length, expressed as nanometers.

Table 1. Reference Value Mean Size and Expanded Uncertainty[(a)]
Average Particle Size (Diameter), in nanometers

Technique	**Analyte Form**	**Particle Size (nm)**
Atomic Force Microscopy	dry, deposited on substrate	55.4 ± 0.3
Scanning Electron Microscopy	dry, deposited on substrate	54.9 ± 0.4
Transmission Electron Microscopy	dry, deposited on substrate	56.0 ± 0.5
Differential Mobility Analysis	dry, aerosol	56.3 ± 1.5
Dynamic Light Scattering	liquid suspension	
backscatter, 173º scattering angle		56.6 ± 1.4
90º scattering angle		55.3 ± 8.3
Small-Angle X-ray Scattering	liquid suspension	53.2 ± 5.3

[(a)] The expanded uncertainties, U, are calculated as $U = ku_c$, where u_c is intended to represent, at the level of one standard deviation, the combined standard uncertainty calculated according to the ISO Guide [2]. The coverage factor, k, for 95 % expanded uncertainty intervals is based on a t multiplier with the appropriate associated degrees of freedom.

Information Values: Information values and associated measurement uncertainties for chemical and electrochemical properties unrelated to particle size are presented in Table 2. NIST information values are considered to be of interest to the RM user, but insufficient information is available to assess adequately the uncertainty associated with the values or a limited number of analyses were performed. Elemental and ion mass fractions and electrochemical properties, including pH, electrolytic conductivity and zeta potential, are listed in Table 2. An optical absorbance spectrum and asymmetric-flow field flow fractionation (AFFF) trace are provided in Figures 1 and 2, respectively. Material sterility and endotoxin content were assessed. Electron microscopy images are provided in Figure 3. Particle size histograms are provided in Figures 4 through 7. Information values cannot be used to establish metrological traceability.

Table 2. Information Value Mean and Measurement Uncertainty[a]
Chemical and Electrochemical Properties

Measurement	Value		
Au mass fraction (μg g^{-1}) [b]	51.86	±	0.64
Cl^- ion mass fraction (μg g^{-1}) [c]	36.3	±	1.2
citrate ion mass fraction (μg g^{-1}) [c]	< 0.02		
Na mass fraction (μg g^{-1}) [d]	--		
pH [e]	7.30	±	0.32
electrolytic conductivity, κ (μS cm^{-1}) [f]	241.6	±	6.5
zeta potential (mV) [g]	-37.6	±	3.0
electrophoretic mobility (μm cm V^{-1} s^{-1})	-2.67	±	0.21

[a] For pH, conductivity and Au mass fraction, the expanded uncertainty (95 % confidence interval) is calculated according to the ISO Guide [2]. Other reported uncertainties are two times the standard deviation of replicate measurements.

[b] Au bound into nanoparticles was determined from separate measurements of total Au and Au dissolved in the solution matrix. Both measurements were made using inductively-coupled plasma optical emission spectrometry (ICP-OES). Total Au was measured after digestion of the particles with a mixture of nitric and hydrochloric acids. Solution matrix Au was measured after removal of Au particles by ultracentrifugation, and was undetectable at the 3σ detection limit corresponding to 0.07 μg g^{-1} in the undiluted supernatant. The Au mass fraction in the matrix was estimated as 0.5 times the 3σ limit and subtracted from the total Au mass fraction to obtain the reported value for the bound Au mass fraction.

[c] Levels of Cl^- and citrate ($C_3H_5O(COO)_3^{3-}$) ions were determined in native suspensions by ion chromatography with a conductivity detector. Chloride and citrate ions were identified based on the retention times of reference standards. Chloride levels in the water blank used to prepare calibrants were insignificant for this analysis. Citrate was not detectable in the water blank. The levels of Cl^- and citrate ions appear to increase slightly as a consequence of centrifugation, but this effect has not been quantified. The limit of detection for citrate is estimated to be 0.02 μg g^{-1}; the limit of quantitation is estimated to be 0.06 μg g^{-1}. Citrate bound to Au particles will not be detected by this approach.

[d] Na mass fraction was determined in the native suspension using inductively-coupled plasma optical emission spectrometry (ICP-OES). Matrix effects and other factors that may affect metrological validity are unaccounted for in this case. Additionally, Na may leach into solution from the inner surfaces of borosilicate glass ampoules. Ongoing studies at NIST have shown that Na mass fractions in excess of 10 μg g^{-1} may result under acidic conditions. The proportion of the observed Na mass fraction that is attributable to leaching is unknown. Furthermore, changes in the Na mass fraction over time are unpredictable. For RM 8013, the Na level detected was within the range that can occur as a result of leaching, and therefore the Na level is not reported.

[e] The pH was determined at 25.0 °C using a combination electrode with ceramic reference junction and a 2 point calibration referred to SRM 186g (pH 6.864) and SRM 187e (pH 9.186).

[f] Electrolytic conductivity was determined at 25.0 °C at 1 kHz using a dip cell with nominal cell constant of 0.1 cm^{-1}. The cell constant was determined using SRM 3191 (nominal κ, 100 μS cm^{-1}) and SRM 3192 (nominal κ, 500 μS cm^{-1}).

[g] Zeta potential was calculated using the Smoluchowski formula from the mean d.c. electrophoretic mobility measured by Doppler velocimetry. For this purpose, a microelectrophoretic light scattering instrument equipped with a quartz capillary cell was used. Measurements were obtained at the cell stationary layer for native suspensions at 20.0 °C after preconditioning the cell with 2 mmol L^{-1} NaCl. Instrument performance was qualified using a vendor supplied –50 mV transfer standard referred to SRM 1980. Since the Smoluchowski formula is intended for systems obeying the thin double-layer approximation, it may not be appropriate for RM 8013 and therefore the mobility value is also provided.

Optical Absorbance: Optical absorbance spectra were obtained using a double-beam spectrophotometer on native suspensions. Measurements were performed using matched quartz cuvettes (10 mm path length) against a filtered deionized water reference. Scan conditions: slit width, 1 nm; scan rate, 240 nm min^{-1}. The coefficient of variation determined near the plasmon peak center was 0.4 % for spectra obtained from 6 randomly selected ampoules. A representative spectrum is presented in Figure 1.

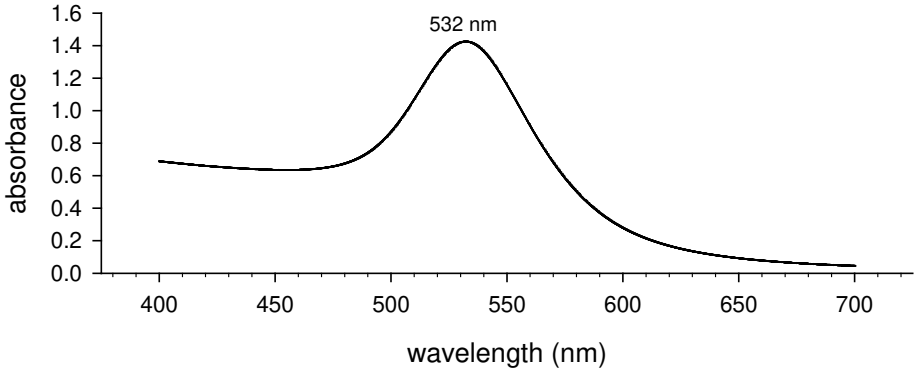

Figure 1. Representative optical absorbance spectrum for the native suspension, centered on the surface plasmon resonance peak for Au. Wavelength of peak maximum is indicated.

Asymmetric-Flow Field Flow Fractionation (AFFF): This representative chromatographic trace was obtained with on-line static light scattering, UV-vis diode array, and DLS detectors under the following conditions: native sample diluted 10-fold in ultrapure deionized water; mobile phase: ultrapure deionized water; membrane: 30 kD polyvinylidenedifluoride (PVDF); channel thickness: 350 µm; channel flow: 0.5 mL min^{-1}; cross flow: 1 mL min^{-1}; injection volume: 100 µL. Peak-center retention time is indicated numerically. Retention time is determined from the endpoint of the focusing step following injection. Duplicate measurements agreed to within 0.01 min peak retention. A representative trace is presented in Figure 2.

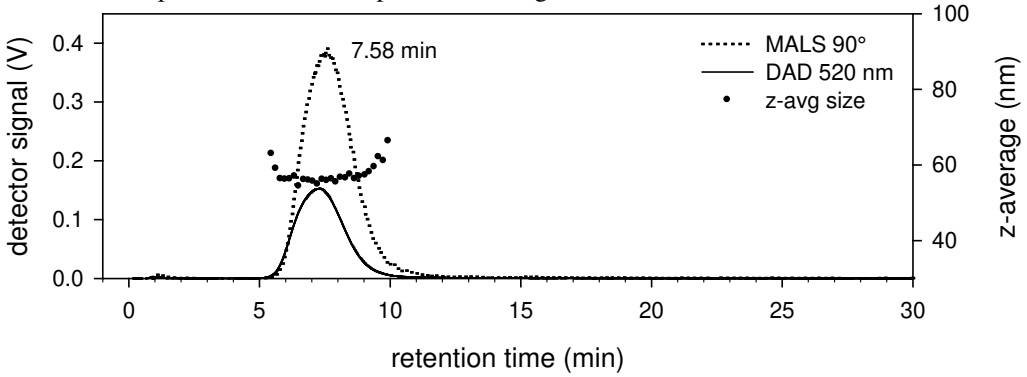

Figure 2. AFFF retention trace showing detector response for 90º light scattering and 520 nm optical absorption. The z-average hydrodynamic diameter values are given across the peak trace.

Sterility and Endotoxin Assessment[1]**:** Sterility was tested by plating RM 8013 on standard Luria-Bertani (LB) culture plates. No colony formation was observed after two days of incubation on LB plates for samples taken before or after sterilization with gamma radiation. Endotoxin was not detected at a level of 2 pg mL^{-1} in samples taken before or after gamma irradiation. [2]

[1] Certain commercial equipment, instruments, or materials are identified in this report in order to adequately specify the experimental procedure. Such identification does not imply recommendation or endorsement by the National Institute of Standards and Technology, nor does it imply that the materials or equipment identified are necessarily the best available for the purpose.

[2] The limulus amoebocyte lysate (LAL) assay was used to detect and measure bacterial endotoxin. Due to interference at the detection wavelength (405 nm) used to quantify the results of the underlying enzymatic reaction, Au particles were removed from the solution by centrifugation at 20,000 g prior to analysis. To test for potential loss of endotoxin due to this procedure, samples of RM 8013 were spiked with lipopolysaccharide (LPS). Spiked samples exhibited some retention; detecting a small absorbance value when subtracting a high background is a potential significant source of uncertainty for these test results. Additionally, this assay cannot exclude the presence of endotoxin previously adsorbed to the Au particles and removed during centrifugation. Samples for analysis were prepared from ampoules randomly selected before and after gamma irradiation.

Electron Microscopy Imaging: Representative micrographs are presented in Figure 3.

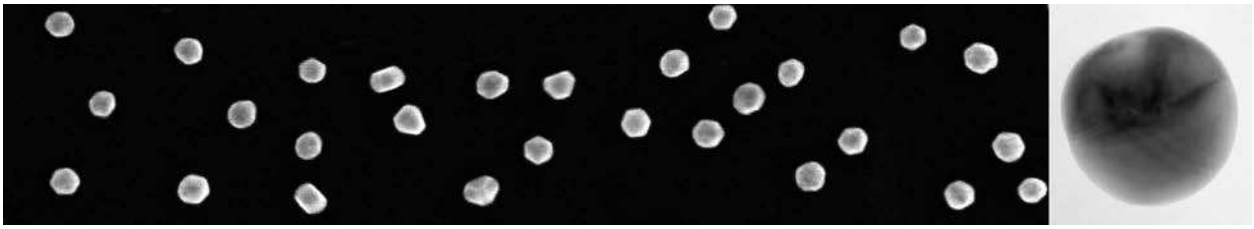

Figure 3. Combined SEM and TEM micrographs. On left: image of Au particles sampled from a single representative SEM scan. On right: high magnification TEM image revealing internal structure and faceting for a single Au particle.

Size Distribution Histograms: Histograms generated by AFM, SEM, TEM and ES-DMA analysis are shown below in Figures 4, 5, 6 and 7, respectively. Binning was performed at a resolution of approximately 1 bin nm^{-1}. Corresponding data sets were used to derive the reported reference values for these methods.

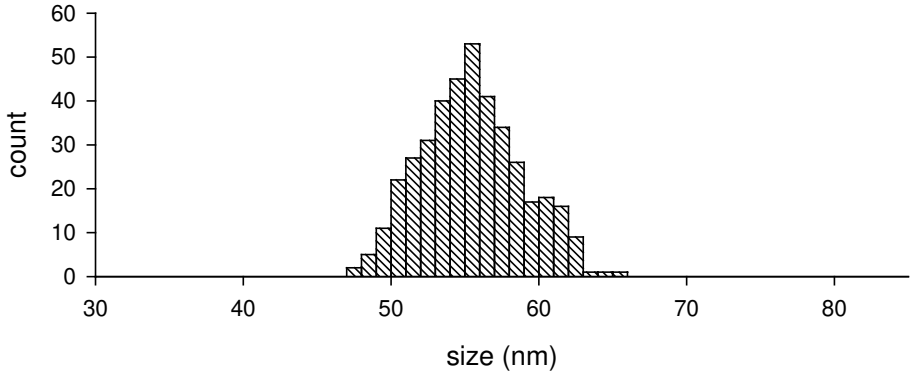

Figure 4. Particle size histogram generated by AFM analysis.

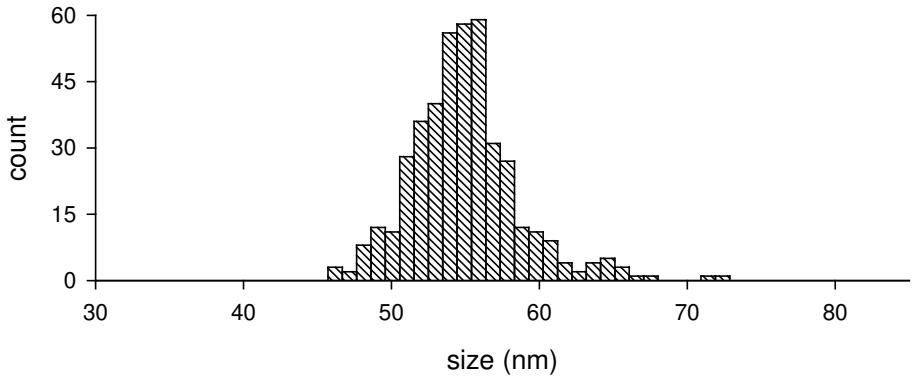

Figure 5. Particle size histogram generated by SEM analysis.

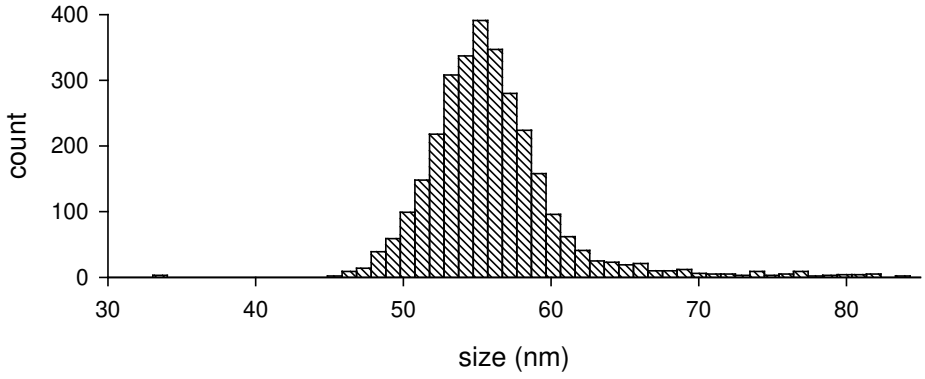

Figure 6. Particle size histogram generated by TEM analysis.

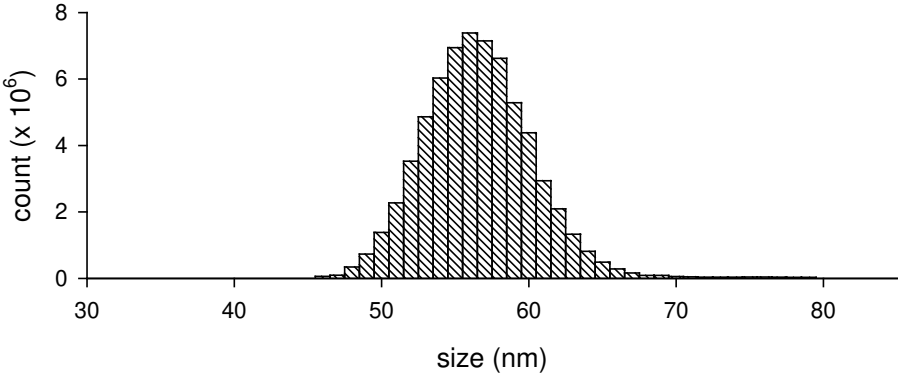

Figure 7. Particle size histogram generated by ES-DMA analysis. Bins containing counts attributable to salt particles have been removed.

NOTICE AND WARNING TO USERS

Handling and Storage: Until required for use, the RM should be **stored at room temperature** in its original ampoule and package, and protected from intense direct light or ultraviolet radiation. Refrigeration is not necessary and is discouraged. Ampoules are best stored long term in a horizontal position. Settling of Au particles is to be expected when the ampoule is left undisturbed for a period of several days or longer, but sediment should resuspend without significantly impacting the size distribution.

Caution: Ampoule contents **should not be allowed to freeze**, as this will permanently compromise the integrity of the material and invalidate reference values. A color change from red-pink to purple or clear indicates that the RM has been compromised. Occasionally, a visible black speck will be observed in an ampoule containing an otherwise translucent red-pink (i.e., normal) solution; this does **not** indicate the sample has been compromised; the specks settle rapidly and can easily be separated from the test material.

Warning: Not for clinical use or human consumption.

INSTRUCTIONS FOR USE

Prior to opening, the glass ampoule containing the RM should be gently inverted several times to insure homogeneity and resuspension of any settled particles. Liquid retained in the upper portion of the ampoule (the nipple), can be dislodged by gently flicking the nipple with forefinger while tilting the ampoule. The ampoule is pre-scored and should be opened by applying moderate pressure with one's thumb to snap off the nipple. It is recommended that the contents of an ampoule be used the same day as opened. Clean laboratory sealing film can be applied to seal a previously opened ampoule for short term storage. If it is necessary to use an ampoule over two or more days, then certain precautions should be taken: opening the ampoule in a clean bench (HEPA filtered) environment using sterile procedures (ethanol rinse), and sealing with ethanol-rinsed laboratory sealing film (optionally, one can transfer the suspension to a clean, sterile plastic or glass vial with a sealing cap), should prolong the useful life of opened ampoules for up to 7 days. Viability after longer term storage cannot be guaranteed, but may be possible if these additional precautions are followed.

PREPARATION AND ANALYSIS

Material Source and Processing: The material used to produce RM 8013 was purchased from BB International of Cardiff, UK. A colloidal Au suspension was prepared to NIST specifications using the citrate-reduction method in a single 8 L batch at their manufacturing facility in the UK. The suspension was shipped in 1 L polycarbonate bottles, and recombined at NIST in a sterile protein-free 10 L borosilicate glass flask. Recombination was performed in a HEPA-filtered clean bench using sterile procedures. The suspension was subsequently flame-sealed into Wheaton 5 mL pre-scored USP Type I glass ampoules using an automated process. Prior to use, the ampoules were cleaned with high pressure deionized water and autoclaved, then flushed with argon gas prior to and during filling. The sealed ampoules containing the Au suspension were sterilized with cobalt-60 gamma radiation to a minimum dose of 31.9 kGy by Neutron Products Inc. of Dickerson, MD.

Heterogeneity Assessment: During the filling process, ampoules were stored in boxes numbered 1 through 11, with box number corresponding to fill order. Heterogeneity testing was performed using measurements of optical density (OD) at 520 nm, hydrodynamic size, and relative Au mass fraction. Measurements of OD and hydrodynamic size (determined by DLS), were performed on native solutions. For these measurements, two samples were extracted from each of 11 randomly selected ampoules (one from each box), for a total of 22 samples for each method. The likelihood ratio [3] (to check if a model that ignores the ampoule effect and a model with the ampoule effect are similar) and ANOVA tests conclude that ampoules are homogeneous for hydrodynamic size and OD.

Au content was evaluated using inductively-coupled plasma optical emission spectrometry performed on 4 samples extracted gravimetrically from each of 11 randomly selected ampoules (one from each box). Analysis followed addition of an internal standard, acid digestion, and dilution with high-purity water. Relative Au mass fraction was calculated as relative instrument sensitivity values. Although likelihood ratio and ANOVA tests, for a level of confidence of 95 %, conclude that there is statistically significant heterogeneity present, the largest and smallest ICP-OES relative sensitivity values differ by only approximately 2 %. Thus, the magnitudes of the observed heterogeneities are probably negligible in relation to the intended use of this material.

Value Assignment and Uncertainty Analysis: Analyses to establish reference values were conducted at NIST using best practices as determined independently for each measurement method. Analyses were performed on replicate (typically two) subsamples drawn from randomly selected (typically four) ampoules of material; subsample sizes and methods were left to the discretion of the expert analyst. For AFM and SEM, the reference values are the means of the measurement results, and the uncertainty level is based on a confidence interval approach [2], with an expanded uncertainty calculated as $U = ku_c$, where the combined uncertainty (u_c) is calculated as the estimated standard deviation of the mean and the coverage factor (k) is the expansion factor of 2 based on the Student's t multiplier associated with a level of confidence of 95 %. For TEM, ES-DMA, and DLS, reference values were calculated from the ampoule means and the uncertainty level is based on a prediction interval approach [4], where the combined uncertainty is calculated as the standard deviation of the ampoule means multiplied by $\sqrt{1+1/N}$ (N is the number of ampoules analyzed) and the coverage factor is based on a t multiplier with N-1 degrees of freedom, for a 95 % expanded uncertainty interval. For SAXS, the restricted maximum likelihood (REML) estimation method [5] was used to fit a linear mixed-effects model [6] with average size, between-instrument variability, and within-instrument variability as parameters. The REML estimate for the average size is the reference value and the REML estimates for the variation of results between- and within-instruments are combined using a root sum of squares to obtain a combined standard uncertainty, u_c [2]. The expanded uncertainty displayed is a confidence limit calculated as $U = ku_c$, where k is the expansion factor associated with a level of confidence of 95 %.

METHODS FOR REFERENCE VALUE MEASUREMENTS

Atomic Force Microscopy (AFM): AFM probes the surface forces between a cantilever tip and the sample deposited on a flat substrate. The tip is rastered over the analysis area producing a 3D topographic image. Height measurements can be obtained with sub-nanometer precision. A Veeco Multimode AFM was used for measurements. Height measurements were calibrated using a silicon step-height transfer artifact (SH70-C19-R19) with a value of 68.9 nm ± 0.7 nm (NIST Calibrated-AFM, Precision Engineering Division) following the prescribed procedure for calibration. Intermediate contact ("tapping") mode was used with a Veeco RTESP phosphorus (n) doped silicon cantilever for imaging (resonance frequency 300 kHz, spring constant 40 N m^{-1}). Atomically flat polycrystalline Au on mica was used as a substrate in order to provide a consistent baseline for size measurements with minimal interference from surface roughness.

To prepare samples for analysis, approximately 1 mL aliquots of native suspension from 2 randomly selected ampoules were placed into 1.5 mL microtubes and centrifuged at 5 krpm for 5 min. A portion of the supernatant from each microtube was then removed and replaced with deionized water to obtain a 3-fold dilution of the native suspension. No change in stability of the suspension was observed during this process. A droplet of each diluted suspension was then placed on the Au substrate and dried at 70 °C. The maximum height with reference to the baseline substrate was recorded as the size (diameter) of the Au particle. Images were collected from different areas of the deposited substrate. Height profiles representing 300 particles from one ampoule and 100 particles from the second ampoule were individually analyzed to acquire the size distribution and mean.

Scanning Electron Microscopy (SEM): In SEM the sample is imaged using low-energy secondary electrons in a process that employs a raster-scanned primary beam. An FEI Helios Dual-Beam SEM was used for imaging, with the following conditions: 15 keV accelerating voltage, 86 pA beam current, 30 µs beam dwell time for each image pixel, and 3.5 mm sample working distance. Image contrast and brightness were set so that a good balance between detail and distinction from background was achieved. For scale calibrations of X and Y directions a VLSI Standards NanoLattice sample was used. This artifact was calibrated on NIST's Calibrated Atomic Force Microscope

(C-AFM) by R.G. Dixson of the NIST Precision Engineering Division, who determined a pitch value of 99.98 nm with an uncertainty of 1.5 nm ($k = 2$). Samples were imaged at 250 k× magnification. A digital capture resolution of (2048 × 1886) pixels was used for all images. Under these conditions, a nominal 60 nm particle will yield an area of roughly (100 × 100) pixels.

The software package ImageJ v1.37 (available from the National Institutes of Health: http://rsb.info.nih.gov/ij/) was used for image processing and data analysis. The Otsu threshold algorithm was implemented to produce a binary image in which the particles are white and the background is black. The outlines of particles as traced by ImageJ were used to check the quality of the particle separation from their background in order to discriminate between single particles and aggregates. The area data for each numbered particle as obtained from ImageJ were first converted to an effective spherical diameter value in pixel units, which was then converted to length units (nm) based on the pitch calibration. A total of 425 particles were analyzed on samples prepared from 3 randomly selected ampoules.

Substrates were prepared by placing a drop of aminopropyldimethylethoxysilane (ADMES) on a clean 5 mm × 5 mm Si substrate cleaved from a 100 mm diameter wafer. The untreated wafer supports a thin, native oxide layer. The ADMES was allowed to react for 2 h to 6 h, after which excess silane was rinsed off with isopropanol followed by deionized water. For analysis, the Au particles were then deposited onto the derivatized substrate by contacting with a droplet of native suspension for a period of 1 h to 2 h. The deposited substrate was then rinsed with isopropanol followed by deionized water, and dried by gently blowing with filtered dry nitrogen prior to analysis. Samples were analyzed as deposited; a conductive coating was not required.

Transmission Electron Microscopy (TEM): TEM measures the projected image of particles deposited onto an electron-transparent substrate. Internal structure, as well as surface morphology, may contribute to the image appearance. A Philips EM400T TEM, operating at 120 kV and equipped with an Olympus Cantega bottom mount CCD camera, was used for measurement of deposited samples. Frames were captured at an exposure time of 2 s. The magnification of the microscope/camera system was calibrated using negatively stained catalase crystals and analyzed by the CRISP software package (http://www.calidris-em.com/). TEM images were analyzed in the IgorPro (http://www.wavemetrics.com/) software package using custom macros written by B.M. Vogel of the NIST Polymers Division. Particle size was determined by measuring the contiguous area of pixels that fall within the threshold set for a particular micrograph. This area was then used to determine the equivalent diameter assuming a spherical particle. Therefore, the average particle size does not consider any pronounced faceting. The circularity value, defined as $P^2/4\pi A$ (where P is the particle perimeter and A is its area), approaches 1 for an ideal circle. Particles with circularities of 6 or higher were not counted to minimize aggregate/artifact inclusion in the size analysis.

The substrate consisted of a 3 mm Cu grid with a 10 nm continuous film of silicon monoxide that was functionalized with aminopropydimethylethoxysilane (ADMES). The substrate was prepared by contacting a commercial grid with about 20 µL of ADMES while sealed in a glass vial to trap vapor and prevent evaporation. After 1 h the grids were removed and dip-washed in ethanol and allowed to dry. To prepare a sample for analysis, one droplet (roughly 8 µL) of native Au suspension was placed on a functionalized grid presented on a stud suspended above a reservoir containing water. A cover was placed over the assembly to prevent evaporation of the Au suspension. After 1 h the grids were dip-washed in distilled water and then ethanol to remove any remaining suspension. The grids were then dried at room temperature prior to measurement. A total of 3030 particles were analyzed on grids prepared from 4 randomly selected ampoules.

Electrospray – Differential Mobility Analysis (ES-DMA): In ES-DMA the liquid suspension is first conveyed into the gas phase using electrospray ionization. The resulting droplets pass through a neutralizing chamber where collisions with charged ions reduce the charge to a modified Boltzmann distribution [7]. Consequently, most of the positively charged particles left after the droplets evaporate possess a single net charge. As they dry, residual salts or other nonvolatile impurities encrust the surface. Within the analysis chamber charged particles are attracted to a negatively biased center electrode, while being dragged along by a carrier gas. Particles for which the electrical force balances the drag force pass through a collection slit, after which a condensation particle counter enumerates the number of particles passing through the detector per cubic centimeter of gas flow. Stepping through the voltage yields a particle size distribution. The experimental system used in this study consisted of an electrospray aerosol generator (Model 3480, TSI Inc.), a differential mobility analyzer (Model 3080n, TSI Inc.) and a condensation particle counter (Model 3025, TSI Inc.). The following conditions were used: capillary diameter, nominally 25 µm; electrospray voltage, 1.67 kV to 2.78 kV; CO_2 pressure and flow rate, 6.89×10^4 Pa and 0.2 L min^{-1}; air pressure and flow rate, 2.55×10^4 Pa and 1.0 L min^{-1}; sheath/carrier gas flow rate, 10 L min^{-1}; flow entering the particle counter (supplemented by filtered air), 1.5 L min^{-1}. The baseline cut off value was set at 30 counts to ensure clear separation between peaks and to account for baseline noise.

Conversion of DMA voltages to equivalent diameters and generation of the particle size distribution were achieved using equations and parameters specified by the commercial vendor of the ES-DMA instrumentation. To account for the thickness of any nonvolatile salts encrusted on the surface of the particles, the mode diameter of the salt peak was determined and subtracted from the subsequent particle sizes, after which the number average diameter was calculated for each sample.

From each of 4 randomly selected ampoules, 900 µL of native suspension was transferred to low-binding microfuge tubes and centrifuged for 12 min at 7.6 krpm. Afterwards, 850 µL of clear supernatant was removed and 500 µL of 2 mmol L^{-1} ammonium acetate solution at pH 8 was added to the tube. A vortex mixer was used to re-homogenize samples, which were then subjected to ES-DMA.

Dynamic Light Scattering (DLS): DLS, also known as photon correlation spectroscopy (PCS) and quasi-elastic light scattering (QELS) is a technique in which the random fluctuation of scattered light from a suspension of Brownian particles dispersed in a liquid medium is measured on a timescale of µs. Intensity fluctuations arise from the size-dependent thermally induced motion of the particles and the refractive contrast between the particles and medium. Photon counts are collected and then processed by a correlator to generate an autocorrelation function (ACF) expressed as the correlation coefficient versus correlator delay time. Backscatter DLS measurements were performed using a Malvern Zetasizer-Nano ZS. Measurement parameters were as follows: laser wavelength, 633 nm (He-Ne); scattering angle, 173º; number of sub-runs (typically), 12; 50 % of sub-runs with highest intensity were removed as a dust rejection filter, yielding a total measurement duration for analysis (typically) of 60 s; measurement temperature, 20 ºC ± 0.1 ºC; medium viscosity, 1.0031 mPa s, medium refractive index, 1.330. Measurements at 90º scattering angle were performed using a Malvern Zetasizer 3000HS under conditions identical to those described for backscatter measurements, except as follows: automatic dust rejection routine enabled, 200 µm aperture used before detector, total duration (with sub-runs) typically 300 s to 360 s. ACFs were fit using the cumulants method as defined by IS0 13321:1996(E) [8]. Data points used in the analysis were obtained by selecting a sub-set of points logarithmically spaced (weighted quadratically) and normalizing these by subtracting the baseline. A last point cut-off at 10 % of signal was applied to the fit. From this analysis the z-average effective-sphere hydrodynamic diameter and polydispersity index (PI) were calculated. Qualification of instrument performance was checked using NIST SRM 1964 (Nominal 60 nm Diameter Polystyrene Spheres).

All sample preparation steps were performed within a HEPA-filtered clean bench. For analysis, the native material was diluted 10-fold into 2 mmol L^{-1} NaCl solution; preliminary tests indicated a concentration-dependence of the measured size at lower dilution factors. Diluted Au suspension was passed through a 0.45 µm PVDF membrane that exhibits low affinity for Au. The diluted sample was loaded into a quartz microcuvette (3 mm path length) for backscatter measurements or a glass cuvette (10 mm path length) for 90º measurements. For each instrument, 5 replicate measurements were performed on each sample and the mean result was recorded. Two aliquots (samples) were tested from each of 4 randomly selected ampoules for a total of 8 measurement results (40 individual measurements) from which the reference value was determined.

For measurements at 90º, observation of a secondary decay in the correlation function characterized by a relaxation time of between 20 µs and 40 µs, may indicate the presence of rotational diffusion or another yet unidentified artifact. Rotational contributions to the ACF could bias the results toward smaller sizes, but the magnitude of this bias on the z-average diameter is difficult to quantify.

Small-Angle X-ray Scattering (SAXS): In the SAXS technique, when a well-collimated, monochromatic beam of hard X-rays passes through a material, any namometer-range inhomogeneities in the electron density scatter a small component of the beam into a small solid angle around the incident direction. Scattered intensity, *I*, is typically presented as a function of the modulus of the scattering vector, $Q = (4\pi/\lambda)\sin(\theta/2)$, where λ is the wavelength and θ is the scattering angle. SAXS data contains information regarding the size, shape, concentration and spatial arrangement of nanoscale inhomogeneities (or particles) present.

SAXS measurements were performed on two instruments that rely on different sample and x-ray optic geometries and x-ray sources. In the first case, measurements were obtained using a customized pin-hole collimated SAXS instrument (Rigaku RA-MICR007) with a Mo rotating anode source (Rigaku, Mo-$K\alpha$, λ = 0.73 Å) and a 2D image plate detector. The configuration produced a beam diameter of 300 µm at the sample plane and provided a *Q*-range from 0.01 $Å^{-1}$ to 2.0 $Å^{-1}$. Native suspensions from 2 randomly selected ampoules were loaded into static liquid cells with a path length of 2 mm. Two samples were analyzed from each ampoule along with a filtered deionized water blank. The data were reduced by radially averaging the 2D detector image and normalizing the data to the acquisition time. *Q* was calibrated using silver behenate powder [10], and data were converted to absolute intensity by normalizing with a glassy carbon reference sample (type 2B from Advanced Photon Source, Argonne National Laboratory). The reduced $I(Q)$ data were fit with a hard-sphere model that accounts for polydispersity in the spheres

with a Schulz distribution using software available from the NIST Center for Neutron Research [11]. The mean particle diameter was determined from a χ-parameter minimized Levenberg-Marquardt fitting.

In the second case, measurements were obtained using the synchrotron-based double-crystal Bonse-Hart Ultra-SAXS instrument [11] at sector 32-ID of the Advanced Photon Source, Argonne National Laboratory [12]. In the configuration used, this instrument provided a Q-range from 0.0001 $Å^{-1}$ to 1 $Å^{-1}$ and absolute intensity calibration by primary methods. Raw data were collected in slit-smeared configuration at a beam energy of 11.5 keV (λ=1.078 Å). Scattering curves were corrected for background/matrix scattering by subtracting an appropriate water blank measurement. The slit-smeared scattered intensity data, $I(Q)$, were analyzed within the Igor software platform with an entropy maximization method [13] incorporating a spherical form factor. The macro is available as part of the Irena macro package on the APS web site (http://usaxs.xor.aps.anl.gov/index.html). Native suspensions from 2 randomly selected ampoules were loaded into static liquid cells with a path length of 1 mm. The remaining suspension from these ampoules was combined and loaded into a capillary flow-cell (mean path length 1.31 mm) equipped with a peristaltic pump, for analysis of the material under flowing conditions; flow improves statistical sampling and eliminates potential issues related to x-ray beam damage, bubble formation or particle settling. The beam size used for static cells was 0.4 mm × 0.4 mm and for the flow cell 0.4 mm × 0.8 mm.

A robust reference value is obtained by combining results from these two instruments to produce a single value for mean diameter that incorporates uncertainties due to variations in instrumentation, sample cell, x-ray source, and choice of fitting algorithm. The reference value was calculated from the mean primary component peak values generated by fitting the $I(Q)$ data resulting from each measurement with the assumption of a hard sphere.

REFERENCES

[1] May, W.; Parris, R.; Beck II, C; Fassett, J.; Greenberg, R.; Guenther, F.; Kramer, G.; Wise, S.; Gills, T.; Colbert, J.; Gettings, R.; MacDonald, B.; *Definitions of Terms and Modes Used at NIST for Value-Assignment of Reference Materials for Chemical Measurements*; NIST Special Publication 260-136; U.S. Government Printing Office: Washington, DC (2000); available at: http://www.nist.gov/srm/publications.cfm (accessed July 2015).

[2] JCGM 100:2008; *Evaluation of Measurement Data - Guide to the Expression of Uncertainty in Measurement*; (ISO GUM 1995 with Minor Corrections), Joint Committee for Guides in Metrology (JCGM) (2008); available at http://www.bipm.org/utils/common/documents/jcgm/JCGM_100_2008_E.pdf (accessed July 2015); see also Taylor, B.N.; Kuyatt, C.E.; *Guidelines for Evaluating and Expressing the Uncertainty of NIST Measurement Results*; NIST Technical Note 1297, U.S. Government Printing Office: Washington, DC (1994); available at http://www.nist.gov/pml/pubs/index.cfm (accessed July 2015).

[3] Tamhane, A.C.; Dunlop, D.D.; *Statistics and Data Analysis: From Elementary to Intermediate*; 1st ed., Prentice Hall: Englewood Cliffs, NJ (2000).

[4] Levenson, L.M.; Banks, D.L.; Eberhardt, K.R.; Gill, M.S.; Guthrie, W.F.; Liu, H.K.; Vangel, M.G.; Yen, J.H.; Zhang, N.F.; *J. Res. Natl. Inst. Stand. Technol.*, Vol. 105, pp. 571-579 (2000).

[5] Neter, J.; Kutner, M.H.; Nachtsheim, C.J.; Wasserman, W.; *Applied Linear Statistical Models*; 4th ed., Irwin: Chicago, IL (1996).

[6] Searle, S.R.; Casella, G.; McCulloch, C.E.; *Variance Components*; New York: John Wiley (1992).

[7] Pinheiro, J.C.; Bates, D.M.; *Mixed-Effects Models in S and S-PLUS;* New York: Springer (2000).

[8] Mulholland, G.W.; Donnelly, M.K.; Hagwood, C.R.; Kukuck, S.R.; Hackley, V.A.; Pui, D.Y.H.; *J. Res. Natl. Inst. Stand. Technol.*, Vol. 111, pp. 257-312 (2006).

[9] ISO; *Particle size analysis - Photon correlation spectroscopy*; IS0 13321:1996(E); International Organization for Standardization: Genève, Switzerland (1996).

[10] Gilles, R., Keiderling, U. and Wiedenmann, A. *J. Appl. Cryst.*, Vol. 31, pp. 957-959 (1998).

[11] Kline, S.R., *J. Appl. Cryst.*, Vol. 39, pp. 895-900 (2006).

[12] Ilavsky, J.; Allen, A.J.; Long, G.G.; Jemian, P.R.; *Rev. Sci. Instrum.*, Vol. 73, pp. 1660-1662 (2002).

[13] Use of the Advanced Photon Source was supported by the U. S. Department of Energy, Office of Science, Office of Basic Energy Sciences, under Contract No. DE-AC02-06CH11357.

[14] Potton, J.A.; Daniell, G.J.; Rainford, B.D.; *J. Appl. Cryst.* Vol. 21, pp. 663-668 (1988).

Report Revision History: 24 July 2015 (Change of expiration date; editorial changes); 09 November 2012 (Extension of expiration period; editorial changes); 13 December 2007 (Original certificate date).

Users of this RM should ensure that the Report of Investigation in their possession is current. This can be accomplished by contacting the SRM Program: telephone (301) 975-2200; fax (301) 948-3730; e-mail srminfo@nist.gov; or via the Internet at http://www.nist.gov/srm.